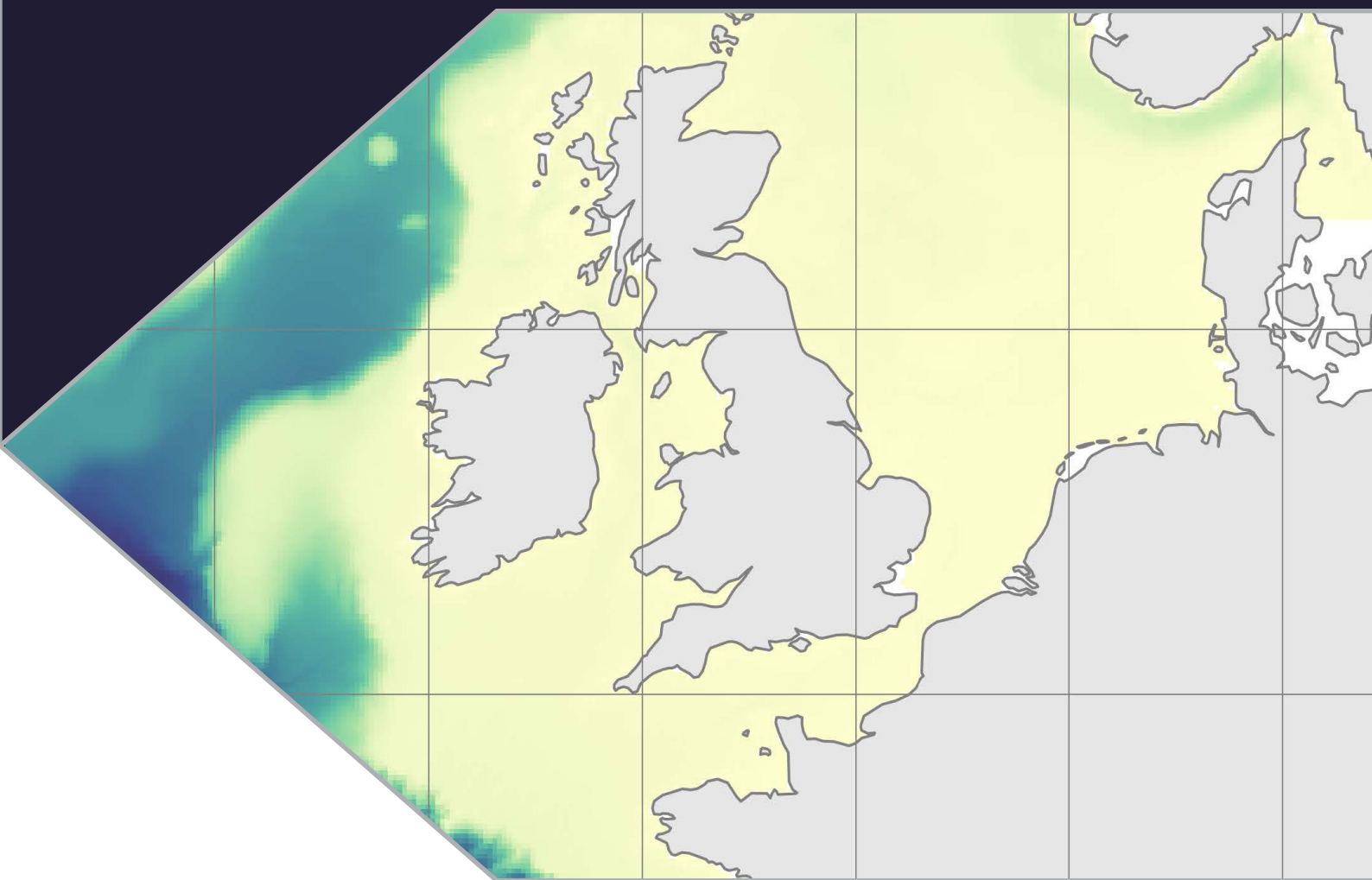


A Reproducible CO9p2 AMM7 NEMOv4.0.4 ERSEM Configuration

Dale Partridge, Yuri Artioli, Helen Powley, and Gennadi Lessin

December 2025



A Reproducible CO9p2 AMM7 NEMOv4.0.4 ERSEM Configuration

Dale Partridge, Yuri Artioli, Helen Powley, and Gennadi Lessin

Plymouth Marine Laboratory

CONTENTS

I	Introduction	1
II	NEMO Configuration	1
II-A	Initial/Boundary Conditions	1
II-B	Tides	1
II-C	Atmospheric Forcing	1
III	ERSEM Configuration	1
III-A	Initial Conditions	2
III-A1	Pelagic Variables	2
III-A2	Benthic Variables	2
III-B	Boundary conditions	2
III-C	Surface Fluxes	4
III-D	River inputs	4

LIST OF FIGURES

1	Atlantic Margin Model 7km domain	1
2	Fitted trends as a function of depth for normalised DIC (top) and TA (bottom) along the Atlantic (left) and Arctic (right) boundaries	4

LIST OF TABLES

I	Initial values for ERSEM pelagic fields. Nitrogen, phosphorus and silicon components are calculated using the Redfield ratio where needed.	3
II	Initial values for ERSEM benthic fields. Values in parentheses indicate a differing value used in the off-shelf area. Nitrogen, phosphorus and silicon components of organic matter are calculated using the Redfield ratio.	3
III	Fixed values applied at the lateral boundaries of the domain. The 'X' in the ERSEM IDs is a wildcard to indicate all variables that satisfy that pattern.	4

A Reproducible CO9p2 AMM7 NEMOv4.0.4 ERSEM Configuration

I. INTRODUCTION

This document describes the setup for the Coastal Ocean Atlantic Margin Model 7km model coupled with ERSEM biogeochemistry. The domain covers the northwest European shelf, reaching the coast of Portugal in the south, Iceland in the north-west and the Skagerrak strait in the east (Fig. 1). With the exception of riverine input, all data and code is open source making this configuration reproducible. Where applicable all scripts and configuration files are available in the PML NEMO project template repository on github: https://github.com/pmlmodelling/NEMO_project_template/tree/AMM7.

II. NEMO CONFIGURATION

The physics configuration closely follows the description discussed in [1], produced by the Joint Marine Modelling Programme (J MMP). The physics configuration repository¹ contains additional source files for NEMO compilation, configuration files to use at runtime along with some general tools to aid producing initial and boundary files.

A. Initial/Boundary Conditions

This configuration is initialised at rest for January 1993. Initial temperature and salinity fields are generated from GloSea6 output, the global ensemble prediction system from the UK Met Office [2]. These fields are first interpolated horizontally onto the AMM7 domain using bilinear interpolation with xESMF[3], followed by a linear interpolation vertically to transform from z -level to σ -level coordinates.

Boundary data (temperature, salinity, east-west and north-south velocities and sea surface height) are also generated from GloSea6 hindcast data using the open source tool pyBDY². There are two boundaries in the setup; one for the open ocean and one for the Baltic, with daily temporal resolution. Configuration files and boundary masks are available in the J MMP repository¹ along with a guide to using the software. Both the oceanic and Baltic open boundaries use GloSea6 data, with a plan to upgrade to using regional model output at the Baltic in the near future.

B. Tides

Tidal forcing is applied at the boundaries, with files generated using the pyBDY tool. 15 tidal constituents are used in the setup (2N2, K1, K2, L2, M2, M4, MU2, N2, NU2, O1, P1, Q1, S1, S2, and T2), created with data using the FES global tidal atlas 2014 (FES2014) [4].

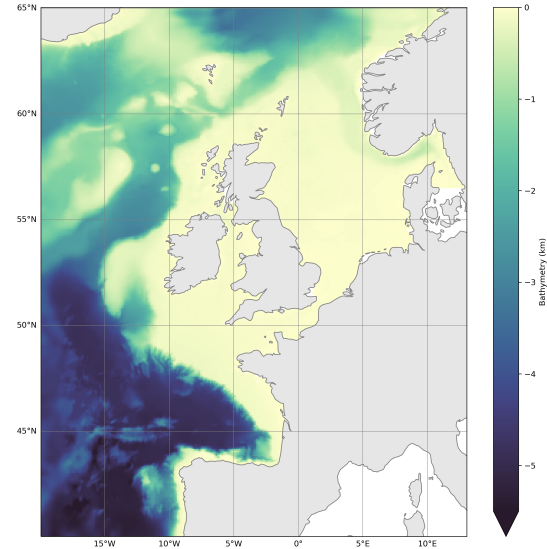


Fig. 1. Atlantic Margin Model 7km domain

C. Atmospheric Forcing

Atmospheric forcing uses data from the ECMWF reanalysis v5 (ERA5) [5]. Eight fields are used: mean sea level pressure, precipitation, longwave radiation flux, shortwave radiation flux, snowfall, 2m air temperature, and 10m winds (u/v). Scripts to download and generate these files are available in the open source tool pySBC³.

III. ERSEM CONFIGURATION

To assign initial and boundary distributions of biogeochemical variables, this version of the ERSEM configuration is designed to either use open source datasets for spatially varying fields, or assign constant values based on experience with other projects. Scripts to produce the input files are available in the companion repository to this document: https://github.com/pmlmodelling/NEMO_project_template/tree/AMM7.

A full description of ERSEM can be found in Butenschön et al. [6]. Since ERSEM has a variable stoichiometry, the Redfield ratio[7] is used extensively to convert between different chemical constituents in the input files, given by:

$$C : Si : N : P = 106 : 15 : 16 : 1 \quad (1)$$

¹[CO9_AMM7_NEMOv4.0.4 Repository](https://github.com/pmlmodelling/NEMO_project_template/tree/AMM7)

²[pyBDY Repository](https://github.com/pmlmodelling/NEMO_project_template/tree/AMM7)

³[pySBC Repository](https://github.com/pmlmodelling/NEMO_project_template/tree/AMM7)

Note that this version of the Redfield ratio is expressed in molar units, whilst ERSEM defines carbon in units of mg .

A. Initial Conditions

The standard ERSEM setup includes 52 pelagic and 36 benthic state variables. An overview of the variables is given in Tables I and II.

1) Pelagic Variables:

Initial values for nutrients (*nitrate, phosphate* and *silicate*), as well as *oxygen* are taken from the 2023 edition of the World Ocean Atlas[8]. This dataset contains monthly records down to 800m, whilst an annual field reaches depths of 5500m. The values below 800m are concatenated to the monthly record matching the start month of the simulation (January), to create a full depth profile. Additionally, *ammonium* is initialised to $0.25 \times nitrate$, although there is high uncertainty associated with this designation.

Dissolved inorganic carbon (DIC) and *total alkalinity* (TA) fields are available through the Global Ocean Data Analysis Project (GLODAP[9]), which provides annual mapped fields for both.

Phytoplankton chlorophyll uses surface total chl-a from Ocean Color Climate Change Initiative (OC-CCI)[10] and is divided into the four PFTs following Brewin et al. [11]. Fields are set uniform down to the pycnocline before exponentially decreasing below. The *phytoplankton carbon* component is derived from the Chl:C ratio used in ERSEM's parameterisation, as shown in Table I, with the remaining constituents calculated through the Redfield ratio (Eq. 1).

Zooplankton is initialised starting from total phytoplankton carbon and assuming a ratio between total zooplankton carbon (Z_c) and total phytoplankton carbon (P_c) of 0.33, based on past numerical experiments in this domain:

$$\sum Z_c = \frac{1}{3} \sum P_c, \quad (2)$$

which is split into meso-zooplankton, micro-zooplankton and heteroflagellates in the ratio 50:10:40 based on prior experiments. The remaining constituents again use the Redfield ratio (Eq. 1).

Dissolved Organic Carbon (DOC) is broken down into the labile ($R1c$), semi-labile ($R2c$) and semi-refractory ($R3c$) components. The labile component is set to a constant value of 12 mgC/m^3 , with the labile dissolved organic nitrogen and phosphorus constituents determined using the Redfield ratio. For semi-labile and semi-refractory DOC, we follow similar assumptions as those used for the Atlantic boundary conditions in Powley et al. [12]: It was assumed that the total surface DOC concentration is $70 \mu\text{M}$ of which we assume $40 \mu\text{M}$ is refractory (not included in ERSEM), $20 \mu\text{M}$ (240 mgC/m^3) is semi-labile and $10 \mu\text{M}$ is semi-refractory (120 mgC/m^3)[13]. Both the semi-labile and semi-refractory are assumed to decrease exponentially with depth, reaching zero by 1000m.

Similar to zooplankton, the total carbon detrital *particulate*

organic matter is initialised based upon approximate January ratios to the total dissolved organic carbon, given by

$$(R4_c + R6_c + R8_c) = \frac{1}{20} (R1_c + R2_c + R3_c), \quad (3)$$

and split into small, medium and large matter in the ratio 70:15:15. Again the Redfield ratios provide the remaining chemical components.

For the remaining variables; the *light absorption* is set to the surface field of ADY as detailed in Section III-C, *calcite* to a constant value of 0.1 mgC/m^3 and *bacteria* carbon to 5 mgC/m^3 . However, bacteria nitrogen and phosphorus are constructed from this using the internal ERSEM maximum ratios to carbon (qnc, qpc) instead of the Redfield ratios.

2) Benthic Variables:

For the benthic variables, due to the scarcity of observational datasets, most have been set to spatially uniform fields based upon previous experiments as shown in Table II. Separate values are applied to the shelf area, defined by a depth less than 200m, and the open ocean area.

The porewater variables *nitrate, ammonium, phosphate, silicate, oxygen* and *DIC* are all given as an approximate equilibrium concentration with the deepest corresponding pelagic field at the bed (depth h), taking into account sediment porosity (p) and benthic layer thickness (z) given by

$$benthic_value = p \times z \times pelagic_value(h). \quad (4)$$

The default ERSEM setup uses values of $p = 0.4$ and $z = 0.3\text{m}$ as standard.

Whilst the pelagic environment generally spin-up relatively quickly, particulate organic matter in the benthos can take many years, even decades to spin up. To improve results, it is recommended to perform consecutive short simulations using the final tracer field as restarts for the beginning of the next simulation. This gives time for the benthic environment to stabilise without drifting too far from the physical conditions at the start of the simulation. Here, six 5-year simulations over 1993-1998 produced a stable set of benthic values to use as the initial conditions for 1993.

B. Boundary conditions

Lateral boundary conditions for biogeochemistry are applied with a monthly resolution.

Nutrients (*nitrate, phosphate* and *silicate*) and *oxygen* data are provided by WOA[8]. As discussed previously the monthly fields are available down to a maximum depth of 800m. In order to achieve both a full depth profile and keep the seasonal variability, the annual fields below 800m have been added to the monthly records before extracting the boundary forcings. These fields are treated as a seasonal climatology.

GLODAP data of *DIC* and *TA* are available as an annual climatological field and are representative of the year 2002 [14]. We know that oceanic DIC has a significant and robust trend due to anthropogenic CO_2 emissions, and it is therefore crucial to represent such a trend (and to a lesser extent any trend in TA) in order to properly represent ongoing acidification

of the shelf environment. For this reason, temporal linear trends from the *in-situ* (cruise) data, collated by GLODAPv2.2020 [15] in the area of the open ocean boundary condition, and normalised to salinity of 35 PSU, have been calculated at various depths, and then an exponential function at depth (h) has been fitted (see 2). Separate trends are calculated for the Arctic and Atlantic boundaries, given by:

$$DIC_{trend} = \begin{cases} 0.77692 \times \exp[-0.000342965h], & \text{Arctic} \\ 0.96805 \times \exp[-0.000519414h], & \text{Atlantic} \end{cases}$$

$$TA_{trend} = \begin{cases} -0.63186 \times \exp[-0.0127709h], & \text{Arctic} \\ 0.18086 \times \exp[-0.000181059h], & \text{Atlantic} \end{cases}$$

These annual trends are applied as a linear function to the climatological values at the boundaries, normalised to a salinity of 35 and centered upon 2002. The normalised values are then converted back to TA and DIC using salinity at the boundaries.

For the Baltic boundary, equations based upon salinity can

	ERSEM ID	Name	Source/Value/Function
Inorganics	$N3_n$	Nitrate	WOA23
	$N4_n$	Ammonium	$0.25 \times N3_n$
	$N1_p$	Phosphate	WOA23
	$N5_s$	Silicate	WOA23
	$O2_o$	Dissolved oxygen	WOA23
	$O3_c$	Dissolved inorganic carbon	GLODAP
	$O3_{TA}$	Total alkalinity	GLODAP
Phyto.	$P1_{chl}$	Diatoms Chl	OC-CCI
	$P1_c$	Diatoms C	$P1_{chl} : P1_c = 0.04$
	$P2_{chl}$	Flagellates Chl	OC-CCI
	$P2_c$	Flagellates C	$P2_{chl} : P2_c = 0.02$
	$P3_{chl}$	Pico-phytoplankton Chl	OC-CCI
	$P3_c$	Pico-phytoplankton C	$P3_{chl} : P3_c = 0.0125$
	$P4_{chl}$	Micro-phytoplankton Chl	OC-CCI
Zoo.	$P4_c$	Micro-phytoplankton C	$P4_{chl} : P4_c = 0.03$
	$Z4_c$	Meso-zooplankton	50% Eq. 2
	$Z5_c$	Micro-zooplankton	10% Eq. 2
Org. Carbon	$Z6_c$	Heteroflagellates	40% Eq. 2
	$R1_c$	Labile Dissolved OC	12 mgC/m^3
	$R2_c$	Semi-labile dissolved OC	240 mgC/m^3 at surface
	$R3_c$	Semi-refractory dissolved OC	120 mgC/m^3 at surface
	$R4_c$	Small particulate OC	70% Eq. 3
Misc.	$R6_c$	Medium particulate OC	15% Eq. 3
	$R8_c$	Large particulate OC	15% Eq. 3
	$light_{ady}$	Light absorption	OC-CCI
Bac.	$B1_c$	Bacteria	5 mgC/m^3
	$L2_c$	Calcite	0.1 mgC/m^3

TABLE I

INITIAL VALUES FOR ERSEM PELAGIC FIELDS. NITROGEN, PHOSPHORUS AND SILICON COMPONENTS ARE CALCULATED USING THE REDFIELD RATIO WHERE NEEDED.

	ERSEM ID	Name	Value/Function
Inorganics	$K3_n$	Nitrate	Eq. 4
	$K4_n$	Ammonium	Eq. 4
	$K1_p$	Phosphate	Eq. 4
	$K5_s$	Silicate	Eq. 4
	$G2_o$	Oxygen	Eq. 4
	$G2_{o_deep}$	Oxygen below zero isocline	0
	$Y2_c$	Deposit Feeders	$3000 (0.1) \text{ mgC/m}^2$
Zoo.	$Y3_c$	Filter Feeders	$1500 (0.1) \text{ mgC/m}^2$
	$Y4_c$	Meiozoobenthos	200 mgC/m^2
	$H1_c$	Aerobic Bacteria	10 mgC/m^2
Bac.	$H2_c$	Anaerobic Bacteria	$100 (1) \text{ mgC/m}^2$
	$Q1_c$	Dissolved OC	$30 (1) \text{ mgC/m}^2$
	$Q6_c$	Slowly Degrading OC	$2000 (500) \text{ mgC/m}^2$
	$Q6_pen_depth$	Average depth Q6 penetrates	$0.03m$
	$Q7_c$	Available Refractory OC	$15 \times Q6$
Org. Carbon	$Q7_pen_depth$	Average depth Q7 penetrates	$0.1m$
	$Q17_c$	Buried Refractory OC	0
	$G3_c$	DIC	Eq. 4
Misc.	ben_nit_G4n	Dinitrogen gas	0 mgN/m^2
	$bL2_c$	Calcite	0.1 mgC/m^2
	ben_col_D1m	Aerobic layer thickness	$0.05 (0.01)m$
Hor.	ben_col_D2m	Reduced layer thickness	$0.25 (0.1)m$

TABLE II

INITIAL VALUES FOR ERSEM BENTHIC FIELDS. VALUES IN PARENTHESSES INDICATE A DIFFERING VALUE USED IN THE OFF-SHELF AREA. NITROGEN, PHOSPHORUS AND SILICON COMPONENTS OF ORGANIC MATTER ARE CALCULATED USING THE REDFIELD RATIO.

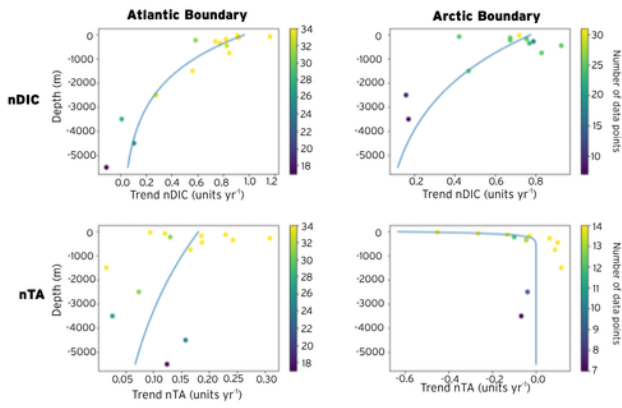


Fig. 2. Fitted trends as a function of depth for normalised DIC (top) and TA (bottom) along the Atlantic (left) and Arctic (right) boundaries

be derived for DIC[16] and TA[17]:

$$DIC = 23.767 \times S + 1388 \quad (5)$$

$$TA = 25.406 \times S + 1410.15 \quad (6)$$

To enable seasonal variability, we assume that DIC/TA seasonality is driven by primary productivity, approximating seasonal fields in terms of nitrate anomalies ($\tilde{N} = N - \bar{N}$) from WOA:

$$DIC = DIC + \frac{106}{16} \tilde{N} \quad (7)$$

$$TA = TA - \tilde{N} \quad (8)$$

where the Redfield ratio is used to convert from nitrogen to carbon for DIC.

As with the initial values, boundary conditions for *semi-labile* and *semi-refractory* DOC exponentially decay from 240/120 mgC/m^3 respectively, down to zero at 1000m, whilst *phytoplankton chlorophyll, nitrogen, phosphate and carbon, zooplankton nitrogen, phosphate and carbon, diatom silicon, particulate organic matter and calcite* use a constant value at the boundaries given in Table III. The decision to impose low values for these variables was made to avoid that the mismatch between the boundary value of nutrients from WOA and a Neumann condition could generate spurious behaviour in biogeochemical relations [18]. Any variable not mentioned here uses a zero-gradient Neumann boundary condition.

C. Surface Fluxes

Biogeochemical surface boundary conditions include nitrogen deposition from the atmosphere, light attenuation due to detritus and yellow substance (gelbstoff absorption coefficient), and atmospheric partial pressure of CO_2 (pCO_2). *Nitrogen deposition* data is available at monthly resolution using models run by EMEP [19], which are then converted into fluxes for both oxidised and reduced components as the sum of both wet and dry deposition.

Atmospheric partial pressure of CO_2 (pCO_2) is available from NOAA [20]. A single global value is provided per month, which is mapped to produce a 2D uniform surface input field.

ERSEM ID	Name	Value/Function
PX_{chl}	Phytoplankton Chlorophyll	$0.0001 \text{ mg}/\text{m}^3$
PX_n	Phytoplankton Nitrogen	$1.26E - 6 \text{ mmolN}/\text{m}^3$
PX_p	Phytoplankton Phosphorus	$7.86E - 8 \text{ mmolP}/\text{m}^3$
PX_c	Phytoplankton Carbon	$0.0001 \text{ mgC}/\text{m}^3$
P_{1s}	Diatom Silicon	$1.18E - 6 \text{ mmolSi}/\text{m}^3$
ZX_n	Zooplankton Nitrogen	$1.26E - 6 \text{ mmolN}/\text{m}^3$
ZX_p	Zooplankton Phosphorus	$7.86E - 8 \text{ mmolP}/\text{m}^3$
ZX_c	Zooplankton Carbon	$0.0001 \text{ mgC}/\text{m}^3$
RX_n	PON	$4.158E - 5 \text{ mmolN}/\text{m}^3$
RX_p	POP	$2.5938E - 6 \text{ mmolP}/\text{m}^3$
RX_c	POC	$0.0033 \text{ mgC}/\text{m}^3$
RX_s	POSi (med/large)	$3.8879E - 5 \text{ mmolSi}/\text{m}^3$
$L2_c$	Calcite	$0.0001 \text{ mg}/\text{m}^3$

TABLE III
FIXED VALUES APPLIED AT THE LATERAL BOUNDARIES OF THE DOMAIN. THE 'X' IN THE ERSEM IDs IS A WILDCARD TO INDICATE ALL VARIABLES THAT SATISFY THAT PATTERN.

The gelbstoff absorption coefficient is a constraint on the 3D passive tracer indicating absorption of light due to coloured dissolved organic matter within ERSEM. Data from OC-CCI [10] provides a 2D surface with which to relax the field. OC-CCI data is available at 8-daily resolution for a multitude of wavelengths which are integrated to produce a single broadband field to use as the constraint.

D. River inputs

River input data is the only source of data not available to reproduce from open source information. The current iteration of river input files used in the CMEMS NW European Shelf reanalysis are an updated version of the dataset used in Lenhart et al. [21]. The dataset is combined with a climatology of daily discharge data from the Global River Discharge Data Base [22] and data prepared by the Centre for Ecology and Hydrology [23]. These files contain time varying daily river discharge, nutrient loads (nitrate, ammonia, phosphate and silicate), total alkalinity, dissolved inorganic carbon and oxygen, and can be made available upon request.

REFERENCES

- [1] Anthony Wise et al. “The effect of vertical coordinates on the accuracy of a shelf sea model”. In: *Ocean Modelling* 170 (2022), p. 101935. ISSN: 1463-5003. DOI: <https://doi.org/10.1016/j.ocemod.2021.101935>. URL: <https://www.sciencedirect.com/science/article/pii/S1463500321001827>.
- [2] D. Storkey et al. “UK Global Ocean GO6 and GO7: a traceable hierarchy of model resolutions”. In: *Geoscientific Model Development* 11.8 (2018), pp. 3187–3213. DOI: [10.5194/gmd-11-3187-2018](https://doi.org/10.5194/gmd-11-3187-2018). URL: <https://gmd.copernicus.org/articles/11/3187/2018/>.
- [3] Jiawei Zhuang et al. *pangeo-data/xESMF*: v0.8.10. 2025. DOI: <https://doi.org/10.5281/zenodo.15304267>.
- [4] F. H. Lyard et al. “FES2014 global ocean tide atlas: design and performance”. In: *Ocean Science* 17.3 (2021), pp. 615–649. DOI: [10.5194/os-17-615-2021](https://doi.org/10.5194/os-17-615-2021). URL: <https://os.copernicus.org/articles/17/615/2021/>.

[5] H. Hersbach et al. *ERA5 hourly data on single levels from 1940 to present*. Copernicus Climate Change Service (C3S) Climate Data Store (CDS), DOI: 10.24381/cds.adbb2d47. 2023.

[6] M. Butenschön et al. “ERSEM 15.06: a generic model for marine biogeochemistry and the ecosystem dynamics of the lower trophic levels”. In: *Geoscientific Model Development* 9.4 (2016), pp. 1293–1339. DOI: 10.5194/gmd-9-1293-2016. URL: <https://gmd.copernicus.org/articles/9/1293/2016/>.

[7] Mark A. Brzezinski. “The Si:C:N ratio of marine diatoms: Interspecific variability and the effect of some environmental variables”. In: *Journal of Phycology* 21.3 (1985), pp. 347–357. DOI: <https://doi.org/10.1111/j.0022-3646.1985.00347.x>.

[8] James R. Reagan et al. *World Ocean Atlas 2023*. NOAA National Centers for Environmental Information. 2024.

[9] A. Olsen et al. “The Global Ocean Data Analysis Project version 2 (GLODAPv2) – an internally consistent data product for the world ocean”. In: *Earth System Science Data* 8.2 (2016), pp. 297–323. DOI: 10.5194/essd-8-297-2016.

[10] S Sathyendranath et al. “An ocean-colour time series for use in climate studies: the experience of the Ocean-Colour Climate Change Initiative (OC-CCI). *Sensors*: 19, 4285.” In: *Sensors* (2019). DOI: [doi:10.3390/s19194285](https://doi.org/10.3390/s19194285).

[11] Robert J. W. Brewin et al. “A three-component model of phytoplankton size class for the Atlantic Ocean”. In: *Ecological Modelling* 221.11 (June 2010), pp. 1472–1483. DOI: 10.1016/j.ecolmodel.2010.02.014.

[12] Helen Powley et al. “Modelling terrigenous DOC across the north west European Shelf: Fate of riverine input and impact on air-sea CO₂ fluxes”. In: *Science of The Total Environment* 912 (Nov. 2023), p. 168938. DOI: 10.1016/j.scitotenv.2023.168938.

[13] Craig A. Carlson and Dennis A. Hansell. “Chapter 3 - DOM Sources, Sinks, Reactivity, and Budgets”. In: *Biogeochemistry of Marine Dissolved Organic Matter (Second Edition)*. Ed. by Dennis A. Hansell and Craig A. Carlson. Second Edition. Boston: Academic Press, 2015, pp. 65–126. ISBN: 978-0-12-405940-5. DOI: <https://doi.org/10.1016/B978-0-12-405940-5.00003-0>. URL: <https://www.sciencedirect.com/science/article/pii/B9780124059405000030>.

[14] S. K. Lauvset et al. “A new global interior ocean mapped climatology: the 1 × 1 GLODAP version 2”. In: *Earth System Science Data* 8.2 (2016), pp. 325–340. DOI: 10.5194/essd-8-325-2016. URL: <https://essd.copernicus.org/articles/8/325/2016/>.

[15] A. Olsen et al. “An updated version of the global interior ocean biogeochemical data product, GLODAPv2.2020”. In: *Earth System Science Data* 12.4 (2020), pp. 3653–3678. DOI: 10.5194/essd-12-3653-2020. URL: <https://essd.copernicus.org/articles/12/3653/2020/>.

[16] Helmuth Thomas and Bernd Schneider. “The seasonal cycle of carbon dioxide in Baltic Sea surface waters”. In: *Journal of Marine Systems* 22.1 (1999), pp. 53–67. ISSN: 0924-7963. DOI: [https://doi.org/10.1016/S0924-7963\(99\)00030-5](https://doi.org/10.1016/S0924-7963(99)00030-5). URL: <https://www.sciencedirect.com/science/article/pii/S0924796399000305>.

[17] Sofia Hjalmarsson et al. “Distribution, long-term development and mass balance calculation of total alkalinity in the Baltic Sea”. In: *Continental Shelf Research* 28.4 (2008), pp. 593–601. ISSN: 0278-4343. DOI: <https://doi.org/10.1016/j.csr.2007.11.010>. URL: <https://www.sciencedirect.com/science/article/pii/S0278434307003123>.

[18] J. Polton et al. “Reproducible and relocatable regional ocean modelling: fundamentals and practices”. In: *Geoscientific Model Development* 16.5 (2023), pp. 1481–1510. DOI: 10.5194/gmd-16-1481-2023. URL: <https://gmd.copernicus.org/articles/16/1481/2023/>.

[19] D. Simpson et al. “The EMEP MSC-W chemical transport model - technical description”. In: *Atmospheric Chemistry and Physics* 12.16 (2012), pp. 7825–7865. DOI: 10.5194/acp-12-7825-2012. URL: <https://acp.copernicus.org/articles/12/7825/2012/>.

[20] X. Lan, P. Tans, and K.W. Thoning. *Trends in globally-averaged CO₂ determined from NOAA Global Monitoring Laboratory measurements*. 2025. DOI: <https://doi.org/10.15138/9N0H-ZH07>.

[21] Hermann-J. Lenhart et al. “Predicting the consequences of nutrient reduction on the eutrophication status of the North Sea”. In: *Journal of Marine Systems* 81.1 (2010). Contributions from Advances in Marine Ecosystem Modelling Research II 23–26 June 2008, Plymouth, UK, pp. 148–170. ISSN: 0924-7963. DOI: <https://doi.org/10.1016/j.jmarsys.2009.12.014>. URL: <https://www.sciencedirect.com/science/article/pii/S0924796309003522>.

[22] C. J. Vörösmarty et al. “Global system of rivers: Its role in organizing continental land mass and defining land-to-ocean linkages”. In: *Global Biogeochemical Cycles* 14.2 (2000), pp. 599–621. DOI: <https://doi.org/10.1029/1999GB900092>.

[23] E. F. Young and J. T. Holt. “Prediction and analysis of long-term variability of temperature and salinity in the Irish Sea”. In: *Journal of Geophysical Research: Oceans* 112.C1 (2007). DOI: <https://doi.org/10.1029/2005JC003386>.